

tions coupling all possible particle occupancy configurations [12]. For $N > 3$, lattice simulations describing the pore dynamics are implemented by choosing a site i and finding the instantaneous current between i and $i+1$: $\hat{J}_i = \hat{p}_i(1 - \hat{q}_{i+1})(1 - \hat{q}_{i+1}^0) - \hat{q}_{i+1}(1 - \hat{p}_i)(1 - \hat{p}_i^0)/2f_0$; $1/g$, where $\hat{p} = 1$ with probability pdt , and zero with probability $(1-p)dt$ as $dt \rightarrow 0$. Analogous expressions hold for the distribution of \hat{q} . The occupations $\hat{p}_i; \hat{q}_i^0$ are then updated and the next particle randomly chosen. An analogous rule holds for \hat{J}^0 . Boundary site kinetics are correspondingly determined by $\hat{p}_N; \hat{q}_N^0$, e.g. $\hat{J}_N = \hat{p}_N(1 - \hat{q}_{N+1})(1 - \hat{q}_{N+1}^0)$. Typically $10^9 - 10^{11}$ steps are needed for $\hat{J}; \hat{J}^0$ to converge to their steady state values, J and J^0 . We verified all results by comparing simulations for both $\hat{p} = \hat{p}^0 = \hat{q} = \hat{q}^0 = 0$ with exact results [11] and general kinetic parameters with numerical results for $N = 3$ [12].

Since particle fluxes across microscopic channels are $< 10^9/s$ [3,4], typical fluid particles suffer $> 10^6$ "collisions" and relax to local thermodynamic equilibrium (LTE) while traversing the pore. Kinetic rates, $f; g; \hat{p}; \hat{q}$, under LTE take Arrhenius forms:

$$\begin{aligned} p' &= q' = (v_T^0)^{-1} \exp(-E_p/k_B T) \\ \hat{p}' &= \hat{q}' = (v_T^0)^{-1} \exp(-E_p/k_B T) \\ \hat{p}; \hat{q} &= \hat{p}^0 \exp(-E_p/k_B T); \end{aligned} \quad (1)$$

with

analogous expressions for $f^0; g^0; \hat{p}^0; \hat{q}^0; \hat{p}^0; \hat{q}^0$. We have for simplicity assumed microscopically symmetric pores and equal hydrostatic pressures (i.e. $\hat{p} = \hat{q}$; $\hat{p}^0 = \hat{q}^0$; $\hat{p} = \hat{q}^0 = \hat{p}^0 = \hat{q}$ when transmembrane potentials $V = 0$ and $V^0 = 0$, respectively) and also that within a narrow pore, particles equilibrate with the pore interior and relax momentum much faster than particle positions, implying, in the absence of external potentials, $\hat{p}' = \hat{q}'; \hat{p}^0' = \hat{q}^0'$. The hopping rates $\hat{p}; \hat{q}$ given in (1) represent ballistic travel times (thermal velocity v_T divided by section length), weighted by internal interaction energies E_p . The entrance energy dependent factors $(\hat{p}; \hat{q})$ and $(\hat{p}^0; \hat{q}^0)$, when multiplied by the relevant number fraction of entering particles, $(\hat{p}_L; \hat{q}_R)$ and $(\hat{p}_L^0; \hat{q}_R^0)$, respectively, define entrance rates into empty boundary sites. The precise values of the prefactors $\hat{p}_0; \hat{q}_0$ will also depend on equilibrium parameters in the reservoirs such as temperature, total number density, and the effective area of the pore mouths. The energy barriers experienced during single particle transport are enumerated in 1(b) and (c) and may include external potentials. If say, the B-particles have charge ze and are acted upon by a ponderomotive transmembrane potential $V^0 \neq 0$, the energy barriers are shifted: $E_p^0 \rightarrow E_p^0 + k_B T v^0/2$ and $E_p^0 \rightarrow E_p^0 - k_B T v^0/2$, where $v^0 = zeV^0/(N+1)k_B T$. Thus, the kinetic rates when $v^0 \neq 0$ are

$$\begin{aligned} (\hat{p}^0; \hat{q}^0; \hat{p}^0) &\rightarrow (\hat{p}^0; \hat{q}^0; \hat{p}^0) e^{-v^0/2} \\ (\hat{p}^0; \hat{q}^0; \hat{q}^0) &\rightarrow (\hat{p}^0; \hat{q}^0; \hat{q}^0) e^{+v^0/2} \end{aligned} \quad (2)$$

When A (B) is uncharged (charged), $J; J^0$ are computed using the parameters $f; g; f_v^0; g_v^0 = (\hat{p}_v; \hat{q}_v; \hat{p}_v^0; \hat{q}_v^0; \hat{p}_v^0; \hat{q}_v^0)$, and $\hat{p}_L^0; \hat{q}_R^0$.

Under isobaric, isothermal conditions, $E(P_L = P_R) = E + E - E - E = 0$, and since pressure fluctuations in liquid mixtures equilibrate much faster than concentration fluctuations, the total enthalpy change per A (B) particle translocated is $H - H^0 - V - V^0$. The efficiency of using species j to pump k can be defined as the ratio of the average free energy gained by k to the free energy lost by j :

$$\eta_{jk} = 1 - \frac{(J^j - J^j_0) - (J^k - J^k_0)}{(J^j - J^j_0)} \frac{J^k(\hat{p}_L^0; \hat{q}_R^0) - J^k_0}{J^j(\hat{p}_L^0; \hat{q}_R^0) - J^j_0}; \quad (3)$$

The Heaviside functions represent the definition that flow is considered useful work only when j and k are co-flowing. Using the entropy of mixing per particle $S^0 = k_B \ln(\hat{p}_L^0; \hat{q}_R^0)$, the Gibbs free energy change per particle, $\Delta G^0 = H^0 - T S^0$, is

$$\Delta G^0 = k_B T \ln \frac{\hat{p}_R^0}{\hat{p}_L^0} + V^0; \quad (4)$$

with an analogous expression for ΔG^0 associated with the transport of an A-type particle. When concentration changes are not too large, higher interaction terms contributing to $H; H^0$ (and hence ΔG^0) can be neglected. These correction terms (which are higher order polynomials in $\hat{p}; \hat{q}$) can be straightforwardly incorporated by independently measuring bulk liquid heats of mixing. For concreteness, we assume species $j = B$ (charged) is used to pump $k = A$ (uncharged) and that for liquids under ambient conditions $v_T = 1 \text{ ps}^{-1}$. Upon setting the time scale $dt = 10 \text{ fs}$, $p = q = p^0 = q^0 = 0.01$.

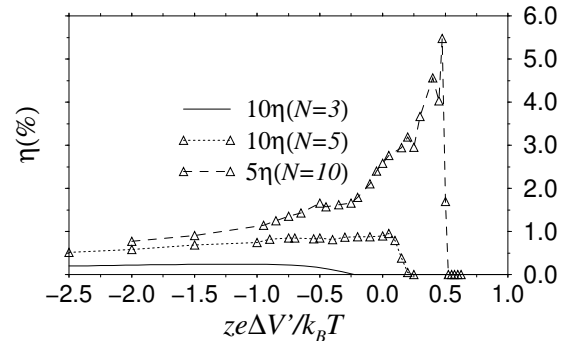


FIG. 2. $10\eta(N=3)$ (exact, solid curves), $10\eta(N=5)$, and $5\eta(N=10)$ as functions of V^0 . The corresponding parameters (for a B-attracting pore) are $\hat{p} = \hat{q} = p = p^0 = q = q^0 = 0.01$ ($dt = 10 \text{ fs}$), and $\hat{p}_L^0 = \hat{q}_R^0 = 0.003$. The intrinsic entrance rates here are $\hat{p}_0 = \hat{q}_0 = \hat{p}^0_0 = \hat{q}^0_0 = 0.01$. The smaller $\hat{p}_0 < \hat{p}; \hat{q}_0$ correspond to a pore that is more attractive to B than to A. Here, $\hat{p}_L^0 = \hat{q}_R^0 = (1 - \hat{p}_L) = (1 - \hat{q}_R) = 0.0036 = 0.0018$, correspond to a 200mM/100mM aqueous B solution in $(L)=(R)$. The computed currents and efficiencies are low and (numerically) noisy due to low (physiological) concentrations \hat{p}_0 , and entrance probabilities \hat{p}_0^0 .

Fig. 2 shows currents and efficiency as functions of a transmembrane potential difference $V^0 \neq 0$, for various length pores. Note that under the physiological conditions considered, the efficiencies are small ($\sim 1\%$) for pores of molecular lengths. A small j^0_j would increase efficiency via transport energetics; however, for too large a V^0 , the B-particles are driven back against their number gradient, and useful work precipitously vanishes. This occurs most easily for short channels where internal A-B interactions are rare; here $V^0 < 0$ is required for B to drive A uphill. The efficiency is non-monotonic and has a maximum as V^0 is varied for fixed f_j^0 and $\frac{0}{L,R}$.

For $V^0 \rightarrow 1$, an asymptotic form for the efficiency can be found by assuming the B particles never hop against the potential gradient,

$$(V^0 \rightarrow 1) \rightarrow -\frac{k_B T}{j^0_j V^0_j} \ln \frac{1 - \frac{0}{R}}{1 - \frac{0}{L}} e^{-j^0_j}; \quad (5)$$

Although J^0 , which is dissipating down its electrochemical potential, generally decreases for longer pores, for small V^0 , $J(N=10) > J(N=5) > J(N=3)$ because pumping is more efficient since there is less likelihood that a B particle can drift through without pushing out all the A particles ahead of it.

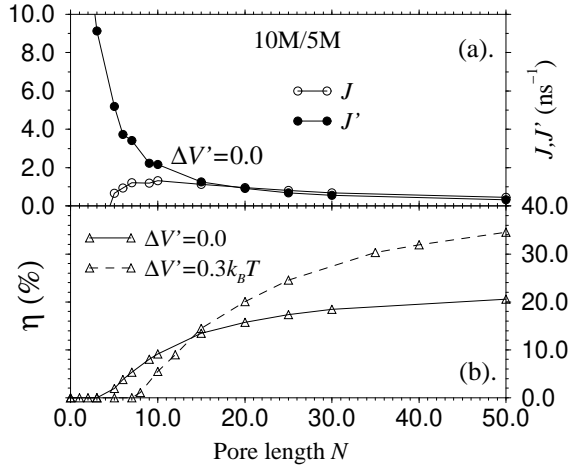


FIG. 3. Dependence of (a). currents and (b). efficiency on pore length $N = L/\lambda$ for $z = V^0 = 0.0; 0.3k_B T$. The parameters f_j^0 used are the same as those in Fig. 2, except $\frac{0}{L} = \frac{0}{R} = 0.18 = 0.09$ corresponding to a 10M/5M aqueous solution. Although $J; J^0$ generally decrease with N , efficiency increases to an asymptotic value.

The particle fluctuations across the pore that allow A and B to simply dissipate their chemical potentials become rarer as membrane thickness or N increases, enhancing efficiency as shown in Fig. 3. Henceforth, unless otherwise indicated, we treat only entropic driving, i.e., $V = V^0 = 0$. Note that $(N = 0; 1) = 0$ is exact for all parameters since $N = 0$ corresponds to an infinitely

thin, noninteracting membrane, and an analytic solution for $J(N=1)/(\frac{0}{R}, \frac{0}{L})$ [11]. When $\frac{0}{R} > 0$, $\frac{0}{R} < \frac{0}{L}$ and $J < 0$, regardless of whether or not solute enters or passes through the single-site pore. This is expected since A and B never interact within the single-site pore for B to be able to "ratchet" A through. For larger N however, we find an asymptotic maximal efficiency defined by the kinetic parameters $f_j^0; g_j^0$. As $N \rightarrow 1$, the large fluctuations required for net particle transport will transfer a constant ratio of A and B particles. This asymptotic efficiency can be tuned by judiciously selecting $f_j^0; g_j^0$ which yield the desired $N \rightarrow 1$ performance. Note that for $V^0 = 0.3$, the $(N \rightarrow 1)$ limit is larger, but for short pores requires larger N both $J; J^0 > 0$ and pumping to take effect, consistent with the results in Fig. 2.

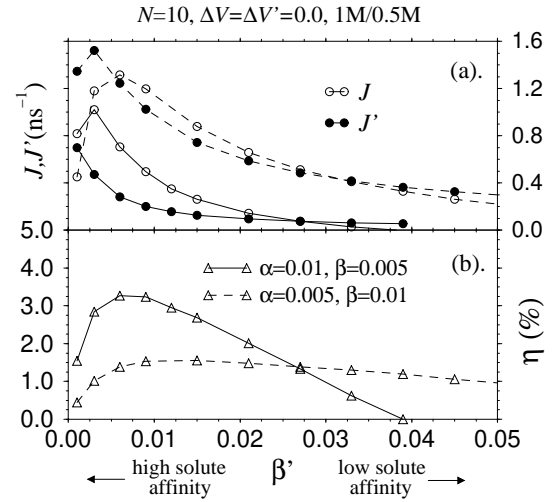


FIG. 4. (a). Currents and (b). efficiency as functions of B-pore binding ($\lambda = \lambda^0$). The solid curves correspond to a slightly A-attracting pore where $\alpha = 0.01; \beta = 0.005$. The dashed curves correspond to an A-repelling pore where $\alpha = 0.005; \beta = 0.01$.

Finally, performance can also be controlled by microscopic pore-molecule interactions. For example, recent simulations have demonstrated dynamic separation factors between species with different pore binding characteristics [14]. We suggest here that similar molecular considerations can be used to design pores [15] that operate as thermodynamic pumps, without moving parts, complex cooperative binding mechanisms [7,16], or external driving forces. Fig. 4 shows the effect of varying B-pore binding $\lambda = \lambda^0$ for two different values of A-pore affinity $\alpha = \alpha^0$.

Pores that do not strongly attract (larger λ^0 [13]), or that repel solutes (smaller λ^0) have lower B particle average occupations $\frac{0}{L}$, and allow solvent (A-particles) to more likely pass from (R) to (L), decreasing efficiency. However, at very small λ^0 (highly attracting pores), $\frac{0}{L}$ increases to the point where it fouls the pore and decreases J relative to J^0 , also decreasing efficiency. Thus, there ex-

ists an intermediate B-pore affinity, which yields a maximum efficiency. Depending on A-pore affinity (dashed vs. solid curves), currents and efficiencies can be simultaneously increased (e.g. by making pores slightly A-repelling when $0.0028 < \phi < 0.004$). These behaviors are a consequence of the intrinsic nonlinearities and are not present in the phenomenological linear Onsager limit [16].

The above results are consistent with, and provide a microscopic theoretical framework for recent anomalous or "negative osmosis" experiments [8]. These measurements show negative osmosis only when the chemical structure of cation exchange membranes was modified by adding CH_2 functional groups. Thus presumably it makes the pores smaller and enhances the likelihood of finite particle size exclusion. More definitively, negative osmosis was measured for a window of fixed membrane charge (CH_2SO_3^-) density. Tuning these fixed counterion charges is equivalent to tuning ϕ for positively charged solutes (solute which exhibited anomalous osmosis were Ca^{+2} , Ba^{+2} , Sr^{+2} , and not H^+ , Na^+) [8]. Figure 4 shows a maximal current and pumping efficiency as a function of ϕ and matches these experimental findings.

There is also evidence for biological manifestations of diffusional pumping [4,9,17]. Recent experiments show that water transport is coupled to Na^+ -glucose [17] and KCl [4] transport. The negative osmotic reflection coefficient measurements across *Necturus* gallbladder epithelia [4] in particular have eluded explanation, although it is conjectured that separate KCl and water transporters must be near each other in the membrane and coupled [4]. However, we have demonstrated how a single simple pore can exchange free energy (even in the absence of direct forces such as transmembrane potentials) between two components and utilize entropy to perform work. This implies that under certain conditions, common membrane channels can mimic symport pumps [6], which are conventionally thought of as more complicated shuttling proteins [2,7,16].

Biological cell membrane channels have sizes that limit diffusional pumping efficiencies, particularly at physiological solute concentrations (Fig. 2). However, the flow rates achievable by simple pores are higher than those of shuttle enzymes and may be a viable mechanism in cellular volume control, or whenever high fluxes are desired. The ubiquity of membrane channels that conduct water [17,4], and are leaky to certain solutes [3,5], suggests the mechanisms presented should be considered when interpreting "negative" osmosis and coupled transport experiments.

We have not treated "slippage," or incomplete coupling processes defined by σ_s which may occur in wider channels and decrease efficiencies. Similarly, attractive interactions between A-A, A-B, and B-B can also affect performance either way. More accurate molecular dy-

namics or Monte-Carlo simulations may reveal further details of diffusion pumping. Systematic measurements, especially on more controllable artificial membrane systems where a wider range of the parameters we have considered can be explored, may eventually reveal secrets of more complicated bioenergetics.

TC was supported by The Wellcome Trust and The National Science Foundation (DM S-98-04780). DL acknowledges support from the DFG through grant Lo556/3-1. We have benefited from discussions with E. D. Siggia, T. J. Pedley, A. E. Hill, and S. B. Hladky. We thank T. H. Her for access to computing facilities.

-
- [1] R. M. Barrer, Zeolites and Clay Minerals as Sorbents and Molecular Sieves, (Academic Press, London, 1978).
 - [2] B. A. Iberts et al., Molecular Biology of the Cell, (Garland, New York, 1994).
 - [3] A. Finkelstein, Water Movement Through Lipid Bilayers, Pore, and Plasma Membranes, (Wiley-Interscience, New York, 1987).
 - [4] T. Zeuthen, Int. Rev. Cytology, 160, 99, (1995); Isotonic Transport in Leaky Epithelia, Eds, Ussing et al., Alfred Benzon Symposium 34, (Munksgaard, Copenhagen, 1993).
 - [5] M. R. Toon and A. K. Solomon, Biophysica et Biochimica Acta, 1063 (2), 179-190A, (1991).
 - [6] A. Su, S. Mager, S. L. Mayo, and H. A. Lester, Biophys. J., 70, 762, (1996).
 - [7] D. G. Nicholls and S. J. Ferguson, Bioenergetics 2, (Academic Press, London, 1992).
 - [8] O. Hahn and D. Wörmann, J. Membrane Sci., 117, 197-206, (1996); J. Schink, H. Rottger, and D. Wörmann, J. Coll. Int. Sci., 171 (2), 351, (1995).
 - [9] W. Y. Gu, W. M. Lai, and V. C. Mow, J. of Biomechanics, 30 (1), 71-78, (1997).
 - [10] B. Derrida, Phys. Reports, 301, 65, (1998).
 - [11] T. Chou, Phys. Rev. Lett., 80 (1), 85, (1998).
 - [12] T. Chou, J. Chem. Phys., 110 (1999).
 - [13] Attractive A-pore affinities are measured by ϕ^1 since E is large and $\exp(-E/k_B T)$ is small. As the pore is made less attractive and eventually repulsive, $E \rightarrow 0$, increases and saturates to ϕ_0 ; eventually, ϕ decreases as E increases (see Fig. 1 (b)). B-pore affinities are similarly defined.
 - [14] L. Xu, M. G. Sedigh, M. Sahini, and T. Totsis, Phys. Rev. Lett., 80 (16), 3511, (1998).
 - [15] V. Russell, C. C. Evans, W. Li, and M. D. Ward, Science, 276, 575, (1997).
 - [16] T. L. Hill, Free energy transduction in biology: the steady-state kinetic and thermodynamic formalism, (Academic Press, New York, 1977).
 - [17] D. Loo, T. Zeuthen, G. Chandy, and E. M. Wright, Proc. Natl. Acad. Sci., 93, 13367, (1996).